

Theoretical determination of stable fourfold coordinated vacancy clusters in silicon

Sangheon Lee and Gyeong S. Hwang*

Department of Chemical Engineering, University of Texas, Austin, Texas 78712, USA

(Received 30 June 2008; published 9 September 2008)

We have identified stable fourfold coordinated vacancy clusters (V_n , $3 \leq n \leq 18$) in Si using a combination of metropolis Monte Carlo, tight-binding molecular-dynamics, and density-functional theory calculations. Our calculations show that the small vacancy defects exclusively favor fourfold coordination thermodynamically rather than hexagonal ringlike structure formation, which has widely been adapted to explain the behavior and properties of vacancy defects. Among those examined, the fourfold V_{12} cluster with S_{22} symmetry is identified to be the most stable, yielding a formation energy of 1.16 eV per vacancy. The fourfold V_{12} structure is about 4 eV more favorable than the conventional hexagonal ring structure. We also discuss how the relative stability between the fourfold and hexagonal ring configurations will change as the cluster size increases to greater than a few tens of vacancies.

DOI: [10.1103/PhysRevB.78.125310](https://doi.org/10.1103/PhysRevB.78.125310)

PACS number(s): 61.72.jd

I. INTRODUCTION

Vacancies are one of the most common native defects in crystalline Si, and can also be generated easily by ion implantation, electron, neutron, and proton irradiations, and plastic deformation. It is now well established that monovacancies are highly mobile in Si even at room temperature,¹⁻³ leading most vacancies to remain in the form of clusters or complexes with other defects and impurities. Earlier experiments based on gold labeling^{4,5} and positron annihilation^{6,7} evidenced the existence of small vacancy clusters. Upon annealing at high temperatures, large open volume defects (greater than a few nanometers in diameter) were also detected by transmission electron spectroscopy.⁸⁻¹¹

Small vacancy defects have been of particular interest because they are a main source or a getter for mobile vacancies and interstitials, which are largely responsible for dopant transient enhanced diffusion and electrical deactivation in ultrashallow junction formation for Si-based electronic devices.¹²⁻¹⁷ Previous theoretical studies¹⁸⁻²¹ proposed “part of hexagonal ring” (PHR) and spherically shaped cluster (SPC) models for the structure of vacancy clusters. According to the models, the V_6 , V_{10} , and V_{14} PHR configurations are predicted to be particularly stable because of their relatively reduced number of Si-Si broken bonds. The PHR and SPC models have also been used to explain large open volume defects.²²⁻²⁷ However, fourfold coordinated V_3 , V_4 , and V_5 clusters were recently identified to be more energetically favorable than their PHR counterparts.²⁸ These fourfold structures were obtained by placing additional Si atoms to terminate dangling bonds in ring hexavacancies. For larger vacancy defects (V_n , $n \geq 7$), no explicit theoretical account is currently available on their stable fourfold coordinated configurations, which could be too complex to be determined by simple trial and error static calculations.

In this work, we establish the structure and formation energies of fourfold vacancy defects in the size range of 3–18 vacancies using a combination of continuous random network model based metropolis Monte Carlo (CRN-MMC), tight-binding molecular-dynamics (TBMD) and density-functional theory (DFT) calculations. The combined ap-

proach has been demonstrated to be an effective means in identifying stable fourfold coordinated defect clusters in Si.^{29,30} We also examine the relative stability between small fourfold and PHR vacancy defects (V_n , $3 \leq n \leq 18$), showing that for each cluster size the identified fourfold structure is energetically more favorable than the conventional PHR structure. The fundamental findings will greatly contribute to a better understanding of the properties of native defects in Si, and their impact on relevant material properties and processing.

II. CALCULATION METHODS

All atomic structures and energies reported herein were calculated using a plane-wave-basis set pseudopotential method within the generalized gradient approximation of Perdew and Wang (GGA-PW91) (Ref. 31) to DFT, as implemented in the well-established VIENNA *Ab Initio* SIMULATION PACKAGE (VASP).³² Vanderbilt-type ultrasoft pseudopotentials³³ were used for core-electron interactions. Outer electron wave functions are expanded using a plane-wave-basis set with a kinetic-energy cutoff of 160 eV. The Brillouin-zone sampling was performed using the ($2 \times 2 \times 2$) Monkhorst-Pack mesh. We used the supercell approach for the defect calculations with a fixed Si lattice constant of 5.46 Å, as obtained from volume optimization. Special care was taken to ensure that each supercell size is large enough to accommodate a given vacancy cluster with no significant interaction with its periodic images. For each defect system, all atoms were fully relaxed using the conjugate gradient method until residual forces on constituent atoms become smaller than 5×10^{-2} eV/Å. For TBMD simulations, semi-empirical potentials developed by Lenosky *et al.*³⁴ were used. A Keating (KT)-like valence bond model was employed for CRN-MMC calculations. Within the Keating-like valence force model, the strain energy (E_{strain}) is given as

$$E_{\text{strain}} = \frac{1}{2} \sum_i k_b (b_i - b_0)^2 + \frac{1}{2} \sum_{i,j} k_\theta (\cos \theta_{ij} - \cos \theta_0)^2,$$

where b_i is the i th bond length and θ_{ij} is the bond angle between bonds i and j , and the equilibrium and force con-

stants are $b_o=2.365$ Å, $\theta_0=109.5^\circ$, $k_b=6.951$ eV/Å², and $k_\theta=1.868$ eV. A detailed description of KT parameter optimization can be found elsewhere.²⁹ Here, it might be worth noting that the values for the two-body (k_b) and three-body (k_θ) force parameters are smaller than 11.976 eV/Å² and 2.097 eV, as optimized for self-interstitial defects.^{29,30} This is due to the fact that vacancy defects are commonly tensily strained while interstitial defects are under compression, and the tensily strained structure is less stiff than the compressively strained one. Hence, the smaller force constants yield a better DFT energetics for vacancy defects. Note that a smaller value of force constant indicates less stiffness in the defect structure.

III. RESULTS AND DISCUSSION

A. Determination of fourfold coordinated vacancy clusters

We first determine the structure and energetics of fourfold-coordinate vacancy clusters in the size range of 3–18 vacancies. For each cluster size, we first generate possible fourfold configurations using CRN-MMC simulations, followed by TBMD simulations at high temperatures (>1000 K) to check their thermal stability. Then, we employ DFT-GGA calculations to refine the geometries of the stable clusters and compare their formation energies to determine the lowest-energy structure among them. The combined approach has been proven to be an effective way to identify stable fourfold-coordinate native defects in crystalline Si.^{29,30} Figure 1 shows the predicted minimum-energy configurations of a few selected fourfold coordinated vacancy defects (V_5 , V_8 , V_{12} , and V_{15}) that exhibit high symmetry. Other configurations are illustrated in Fig. 2.

Compared with previously reported small fourfold vacancy clusters (V_n , $3 \leq n \leq 6$),²⁸ our calculations yield the same configurations for V_3 , V_4 , and V_6 . The previously proposed V_5 structure was obtained by relaxing its conventional PHR state,²⁸ exhibiting a combination of three five-membered and two six-membered rings. On the other hand, as shown in Fig. 1(a), the V_5 structure identified in this work consists of one five-membered, two six-membered, and two seven-membered rings, as typically seen for well-relaxed {311} extended defects.^{35,36} The structure is predicted to be 0.33 eV more favorable than the previous one. It is evident that larger-membered rings are more flexible than smaller ones, which in turn more effectively relieves the defect-induced strain. In addition, we find that the fourfold vacancy clusters commonly contain four-membered or/and five-membered rings, which are preferentially placed in the center region, while surrounded by more flexible larger-membered (seven-membered or/and eight-membered) rings. For instance, as shown in Fig. 1(b) the predicted fourfold V_8 structure with C_{2h} symmetry is composed of two symmetric voids, which face each other with four-membered ring as mirror plane, and each void is surrounded by one four-membered, six six-membered, and two seven-membered rings.

The fourfold vacancy clusters are tensily strained with bond-length deviations of -0.05 – 0.4 Å from the equilibrium value of ≈ 2.36 Å [see Fig. 3]. Analyzing calculated

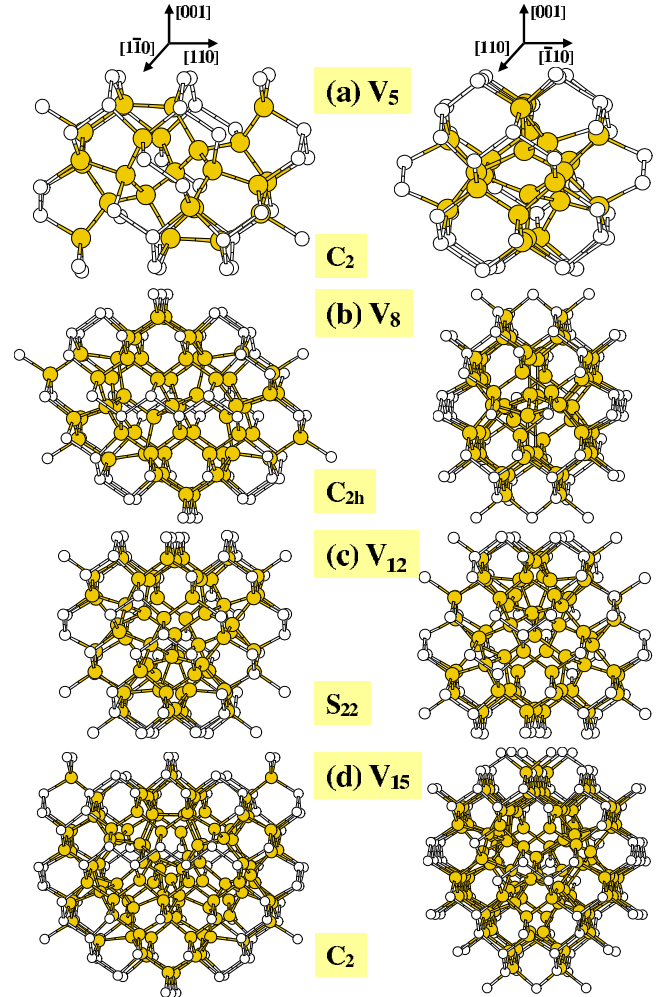


FIG. 1. (Color online) Predicted fourfold configurations for (a) V_5 , (b) V_8 , (c) V_{12} , and (d) V_{15} in Si. Grey (gold) balls indicate more distorted atoms than the rest of the lattice atoms (in white). For each defect, the left and right panels show two different views, as indicated. The symmetry of each defect is also indicated.

maximally localized Wannier functions for the defect configurations, we see that Wannier centers insignificantly, mostly less than 0.1 Å, depart from the midpositions of two bonded atoms [see Fig. 5(a) for the V_{12} case]. The spread of the Wannier functions is also close to that in bulk crystalline Si, confirming fourfold coordination of the vacancy defects. In addition, our density of state analysis shows no energy levels within the Si band gap. This indicates that the fourfold vacancy defects are optically inactive, which may in turn impede their direct characterization using optical and electrical measurements.

B. Relative stability between fourfold and part of hexagonal ring vacancy defects

Figure 4(a) shows the calculated formation energies of small vacancy defects (V_n , $n=3$ –18) in both fourfold and PHR configurations. Here, the formation energy per vacancy is given by $E_f(n) = \{E(N-n) - (1-n/N)E(N)\}/n$, where $E(N-n)$ and $E(N)$ are the total energies of N -atom supercells

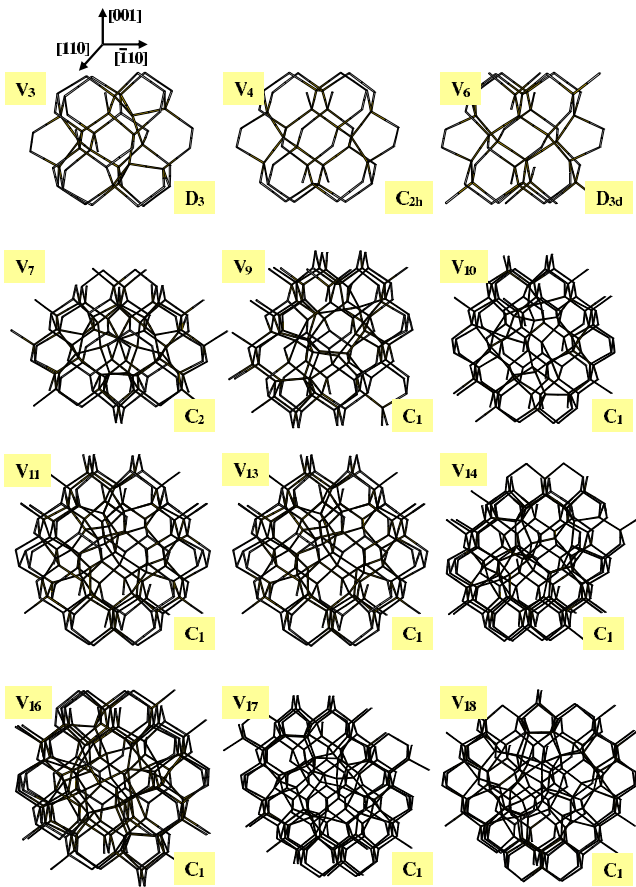


FIG. 2. (Color online) Wireframe illustrations of stable fourfold coordinated vacancy clusters identified in this work (V_n , $n=3-18$; see Fig. 1 for V_5 , V_8 , V_{12} , and V_{15}).

with a n -vacancy cluster and with no defect, respectively. In the inset, the total-energy differences between the fourfold and the PHR states are also presented. For the PHR vacancy clusters, care is taken to ensure possible pairings between

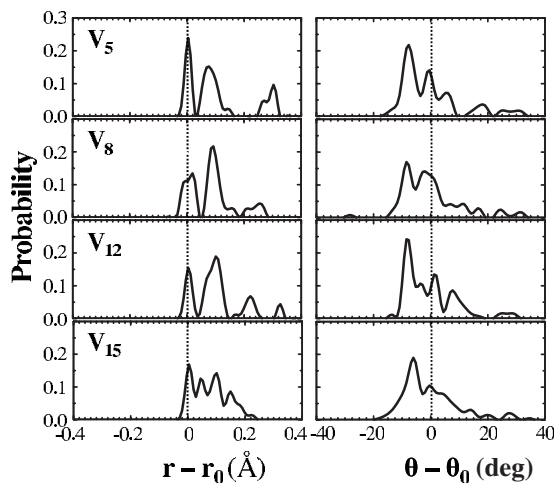


FIG. 3. Distributions of bond length (left panels) and bond angle (right panels) deviations associated with the distorted atoms as shown in Fig. 1. The dotted lines indicate the equilibrium values of $r_0=2.365$ Å and $\theta_0=109.5^\circ$.

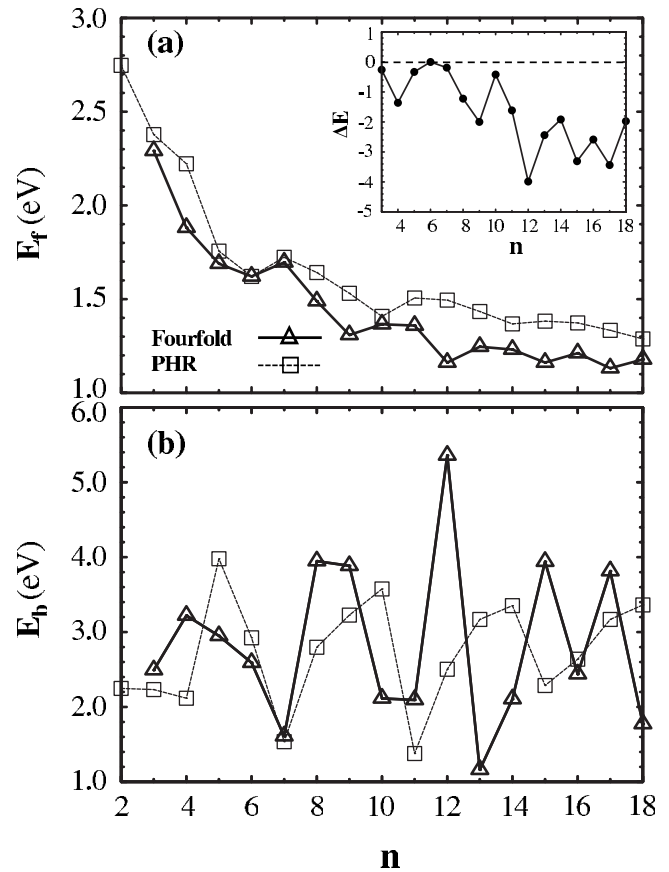


FIG. 4. (a) Calculated formation energies per vacancy (E_f) and (b) binding energies of vacancy clusters as a function of cluster size (n) for both fourfold (indicated as “fourfold”) and PHR (“PHR”) configurations. For the PHR case, the atomic structures from previous studies (Refs. 20 and 21) were recalculated within DFT-GGA. To minimize possible interactions between a defect and its periodic images, we carefully evaluated the formation energies by changing the supercell size; $480-n$ and $576-n$ atom supercells, where n is the number of vacancies, were used for V_1-V_{14} and $V_{15}-V_{18}$, respectively. The inset shows a variation in the total-energy difference (ΔE in electron volts) between the fourfold and PHR cases.

dangling bonds created by removal of Si lattice atoms via structural relaxation using combined CRN-MMC and DFT calculations. The rigorous ionic relaxation leads to reconfiguration of V_5 to a fourfold state as also reported by Makhov and Lewis.²⁸ Given the ease of reconfiguration, here we consider the fourfold structure as the PHR V_5 rather than the conventional PHR structure. Recall that the fourfold PHR state is 0.33 eV less favorable than our identified fourfold structure. For other PHR clusters, there is no significant structural rearrangement. Hence, the ionic relaxation leads to insignificant variations in their formation energies due to the well-known flatness of the total-energy surface of vacancy defects.

For the small vacancy defects, our results demonstrate that the fourfold coordinated configurations are energetically more favorable than the PHR configurations. The energy difference can be as large as 4 eV when $n=12$. While the information related to the fourfold states was lacking, the PHR states have been mostly considered for understanding the

behavior and properties of vacancies. In addition, SPC have also been identified to be stable. Particularly for V_{17} , the SPC was expected to be more favorable than the PHR cluster.²¹ Our DFT-GGA calculation, however, predicts the fourfold V_{17} cluster to be 2.6 eV more favorable than the SPC.

According to our calculations, small vacancy defects thermodynamically favor fourfold coordination in crystalline Si. This is apparently due to the fact that the energy gain by bond formation exceeds the associated strain energy. It is also well established that energetically small self-interstitial clusters (I_n , $n \geq 3$) prefer to be fourfold coordinated.^{29,30} Considering less stiffness in the tensily strained structure compared to the compressively strained one, one can expect that the fourfold coordination of vacancy defects (which are commonly tensily strained) will be energetically more facile than interstitial defects (which are typically under compression). Indeed, as pointed out earlier for the Keating-like valence force model, the two-body force parameters of $k_b = 6.951$ and 11.976 eV/Å² provide the best fit to our DFT energetics for fourfold-coordinate vacancy and interstitial defects, respectively, indicating that the vacancy structures are less stiff. This also explains why the formation energies of fourfold vacancy clusters (see Fig. 4) are commonly lower than those of fourfold interstitial clusters (see Fig. 3 in Ref. 30).

Annealing of vacancy defects may be preceded by dissociation into smaller ones in a vacancy-rich region. Thus, to examine their thermal stability we also calculate the binding energies of the fourfold and the PHR vacancy clusters. The results are summarized in Fig. 4(b). Here, the binding energy is given by $E_b(n) = (n-1)E_f(n-1) + E_f(1) - nE_f(n)$, which represents an energy cost for single vacancy liberation from a given cluster, i.e., $V_n \rightarrow V_{n-1} + V$. For the PHR case, the binding energies show an oscillating behavior with local maxima at $n=5, 10, 14$, and 18 , in good agreement with previous studies²¹ except for V_5 and V_6 . The discrepancy is attributed to the fact that for V_5 we consider the stable fourfold PHR state converted from the conventional PHR (see above), leading to increase in the binding energy of V_5 while lowering the V_6 binding strength accordingly. For the fourfold vacancy clusters, their binding energies are similar in magnitude to those of the PHR clusters although they exhibit local maxima and minima at different sizes.

Among all the defect configurations considered, the fourfold coordinated V_{12} turns out to be the most favorable thermodynamically with a binding energy of 5.36 eV. As shown in Fig. 5(a), the V_{12} structure has S_{22} symmetry with a combination of four identical structural units. The structure of each unit consists of two five-membered, two six-membered, and two eight-membered rings, resembling a small void. The V_{12} structure can be viewed as the V_{17} SPC with a well-relaxed tetragon inside. (The V_{17} SPC is obtained by removing up to the second-nearest neighbors around a center atom). It is worth pointing out that the six bond angles around the center atom (as indicated) are 109.5° , identical to the equilibrium tetrahedral bond angle of crystalline Si. The well-relaxed fourfold structure can also be evidenced by the Wannier centers, which are almost perfectly located at bond midpoints [Fig. 5(a)], as well as the total density of states, which appears virtually identical to that for defect-free Si

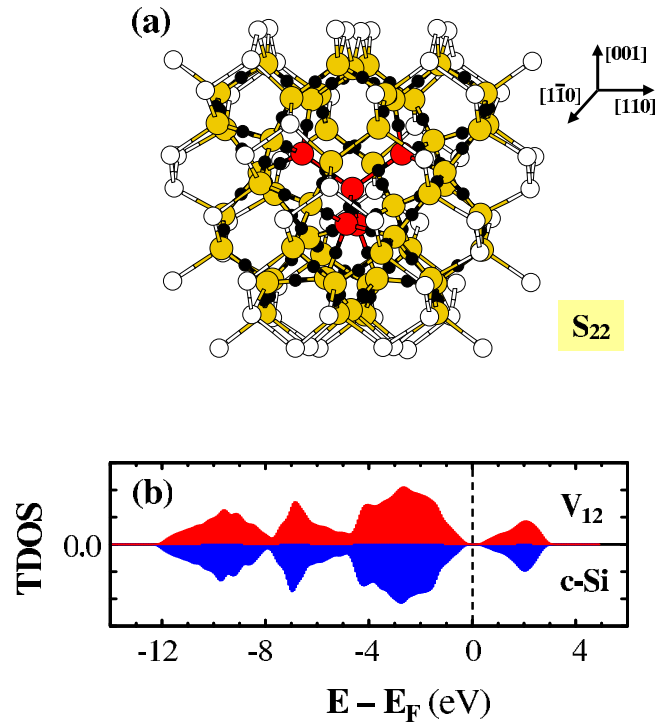


FIG. 5. (Color online) (a) Ball-and-stick illustration of the atomic structure of V_{12} , together with Wannier function centers as indicated by small black balls. Grey (gold) balls indicate more distorted atoms than the rest of the lattice atoms (in white), while five dark gray (red) balls indicate a well-relaxed tetragon at the defect center. (b) Calculated total density of states (TDOS) for the c -Si system with (upper panel) and without (lower panel) the V_{12} cluster. Here, E_F indicates the Fermi level.

[Fig. 5(b)]. Having significant stability, the fourfold V_{12} cluster could be expected to exist to a large extent in a vacancy-rich region although its direct characterization appears impractical at present.

Finally we consider how the relative stability between fourfold and PHR configurations will change as the cluster size increases to greater than a few tens of vacancies. While fourfold coordination appears preferred thermodynamically for small vacancy clusters, earlier transmission electron microscopy (TEM) experiments⁸⁻¹¹ evidenced the formation of open volume defects (of larger than 5 nm in diameter) rather than equivalent-size fourfold defects. This may imply that voidlike defects in the PHR or the SPC structure would become energetically favored when the defect size is sufficiently large. In fact, one can expect that the formation energy of voidlike defects is largely governed by the void-surface energy, which is proportional to the void-surface area ($\sim n^{2/3}$), whereas that of fourfold coordinated defects is determined by the number of strained Si atoms, which is proportional to the cluster size ($\sim n$). As shown in Fig. 6, indeed the calculated formation energies are well fitted with the power $(-0.32 + 3.4n^{2/3})$ and the linear $(4.2 + 0.92n)$ functions, respectively, for the PHR and the fourfold cases. The small defects may not properly represent the general trend, and thus the fitting curves would not precisely describe the formation energy variations of larger vacancy defects. Nonetheless, this approximation should be sufficient to demonstrate

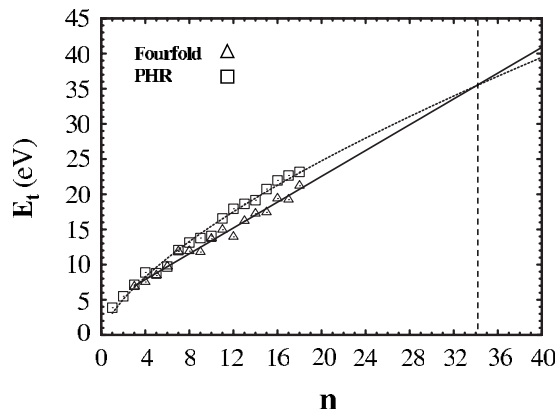


FIG. 6. Prediction of the formation energies of fourfold and PHR vacancy defects as the cluster size (n) increases to greater than a few tens of vacancies, assuming that the former is proportional to the cluster size ($\sim n$) while the latter to the void-surface area ($\sim n^{2/3}$). The DFT values as indicated are well fitted with the linear ($4.2+0.92n$) and the power ($-0.32+3.4n^{2/3}$) functions, for the fourfold and the PHR cases, respectively.

that generally the PHR configuration will be energetically more favorable than the fourfold configuration when the defect size is greater than a couple of nanometers in diameter.

IV. SUMMARY

Based on combined CRN model, TBMD, and DFT calculations, we present stable fourfold coordination for small vacancy clusters in the size range of 3–18 vacancies. For each cluster size, we first generated possible fourfold vacancy clusters using CRN-MMC simulations, followed by TBMD simulations at high temperatures to check the stability of the fourfold structures. Then, DFT calculations were performed

to refine the geometries of the stable clusters, and compared their formation energies to determine the lowest-energy structure among them. For the small vacancy defects, our results demonstrate that fourfold configurations are energetically more favorable than PHR configurations, which have been until now considered to be prevailing. The preference for fourfold structuring is apparently attributed to the fact that the energy gain by bond formation exceeds the strain energy associated. In particular, we identify a very stable fourfold V_{12} structure that consists of four identical structural units while each unit has two five-membered, two six-membered, and two eight-membered rings. The fourfold V_{12} structure is predicted to be about 4 eV more favorable than the conventional PHR structure. Given the significant stability, we expect that the fourfold V_{12} defect would exist to a large extent in a vacancy-rich region. While small vacancy defects thermodynamically favor fourfold coordination in crystalline Si, our theoretical study also demonstrates that the PHR configuration will become energetically more favorable than the fourfold configuration when the defect size is greater than a couple of nanometers in diameter. The improved understanding regarding the structure and stability of vacancy defects will greatly assist in better understanding the properties of native defects in Si, and explaining and predicting their impact on relevant material properties and processing.

ACKNOWLEDGMENTS

We acknowledge Semiconductor Research Corporation (Contract No. 1413-001), the National Science Foundation (Contract No. CAREER-CTS-0449373) and the Robert A. Welch Foundation (Contract No. F-1535) for their financial support. We would also like to thank the Texas Advanced Computing Center for use of their computing resources.

*Author to whom correspondence should be addressed. gshwang@che.utexas.edu

¹G. D. Watkins, *J. Phys. Soc. Jpn.* **18**, 22 (1963).

²J. A. Van Vechten, *Phys. Rev. B* **10**, 1482 (1974).

³S. Coffa and S. Libertino, *Appl. Phys. Lett.* **73**, 3369 (1998).

⁴V. C. Venezia, D. J. Eaglesham, T. E. Haynes, A. Agarwal, D. C. Jacobson, H.-J. Gossmann, and F. H. Baumann, *Appl. Phys. Lett.* **73**, 2980 (1998).

⁵R. Kalyanaraman, T. E. Haynes, V. C. Venezia, D. C. Jacobson, H.-J. Gossmann, and C. S. Rafferty, *Appl. Phys. Lett.* **76**, 3379 (2000).

⁶P. Mascher, S. Dannefaer, and D. Kerr, *Phys. Rev. B* **40**, 11764 (1989).

⁷R. Krause-Rehberg, M. Brohl, H. S. Leipner, T. Drost, A. Polity, U. Beyer, and H. Alexander, *Phys. Rev. B* **47**, 13266 (1993).

⁸D. S. Zhou, O. W. Holland, and J. D. Budai, *Appl. Phys. Lett.* **63**, 3580 (1993).

⁹S. L. Ellingboe and M. C. Ridgway, *Nucl. Instrum. Methods Phys. Res. B* **127-128**, 90 (1997).

¹⁰J. S. Williams, M. J. Conway, B. C. Williams, and J. Wong-

Leung, *Appl. Phys. Lett.* **78**, 2867 (2001).

¹¹A. Peeva, R. Koegler, and W. Skorupa, *Nucl. Instrum. Methods Phys. Res. B* **206**, 71 (2003).

¹²R. A. Brown, D. Maroudas, and T. Sinno, *J. Cryst. Growth* **137**, 12 (1994).

¹³V. C. Venezia, T. E. Haynes, A. Agarwal, L. Pelaz, H.-J. Gossmann, D. C. Jacobson, and D. J. Eaglesham, *Appl. Phys. Lett.* **74**, 1299 (1999).

¹⁴M. T. Zawadzki, W. Luo, and P. Clancy, *Phys. Rev. B* **63**, 205205 (2001).

¹⁵G. S. Hwang and W. A. Goddard III, *Phys. Rev. B* **65**, 233205 (2002).

¹⁶T. A. Frewen, S. S. Kapur, W. Haeckl, W. von Ammon, and T. Sinno, *J. Cryst. Growth* **279**, 258 (2005).

¹⁷D. A. Abdulmalik and P. G. Coleman, *Phys. Rev. Lett.* **100**, 095503 (2008).

¹⁸D. J. Chadi and K. J. Chang, *Phys. Rev. B* **38**, 1523 (1988).

¹⁹J. L. Hastings, S. K. Estreicher, and P. A. Fedders, *Phys. Rev. B* **56**, 10215 (1997).

²⁰A. Bongiorno, L. Colombo, and T. Diaz de la Rubia, *Europhys.*

- Lett. **43**, 695 (1998).
- ²¹T. E. M. Staab, A. Sieck, M. Haugk, M. J. Puska, T. Frauenheim, and H. S. Leipner, Phys. Rev. B **65**, 115210 (2002).
- ²²M. Saito and A. Oshiyama, Phys. Rev. B **53**, 7810 (1996).
- ²³A. La Magna, S. Coffa, and L. Colombo, Phys. Rev. Lett. **82**, 1720 (1999).
- ²⁴G. Amarendra, R. Rajaraman, G. Venugopal Rao, K. G. M. Nair, B. Viswanathan, R. Suzuki, T. Ohdaira, and T. Mikado, Phys. Rev. B **63**, 224112 (2001).
- ²⁵S. Chakravarthi and S. T. Dunham, J. Appl. Phys. **89**, 4758 (2001).
- ²⁶B. P. Haley, K. M. Beardmore, and N. Grønbech-Jensen, Phys. Rev. B **74**, 045217 (2006).
- ²⁷S. Dannefaer, V. Avalos, and O. Andersen, Eur. Phys. J. Appl. Phys. **37**, 213 (2007).
- ²⁸D. V. Makhov and L. J. Lewis, Phys. Rev. Lett. **92**, 255504 (2004).
- ²⁹S. Lee and G. S. Hwang, Phys. Rev. B **77**, 085210 (2008).
- ³⁰S. Lee and G. S. Hwang, Phys. Rev. B **78**, 045204 (2008).
- ³¹J. P. Perdew and Y. Wang, Phys. Rev. B **45**, 13244 (1992).
- ³²G. Kresse and J. Furthmüller, *VASP the guide* (Vienna University of Technology, Vienna, 2001).
- ³³D. Vanderbilt, Phys. Rev. B **41**, 7892 (1990).
- ³⁴T. J. Lenosky, J. D. Kress, I. Kwon, A. F. Voter, B. Edwards, D. F. Richards, S. Yang, and J. B. Adams, Phys. Rev. B **55**, 1528 (1997).
- ³⁵M. Kohyama and S. Takeda, Phys. Rev. B **46**, 12305 (1992).
- ³⁶J. Kim, J. W. Wilkins, F. S. Khan, and A. Canning, Phys. Rev. B **55**, 16186 (1997).